

# Warm non-equilibrium gas phase chemistry as a possible origin of high HDO/H<sub>2</sub>O ratios in hot and dense gases: application to inner protoplanetary discs

W.-F. Thi<sup>1</sup>\*, P. Woitke<sup>2</sup>, I. Kamp<sup>3</sup>

<sup>1</sup>*†SUPA, Institute for Astronomy, University of Edinburgh, Royal Observatory, Blackford Hill, Edinburgh, EH9 3HJ, UK*

<sup>2</sup>*UK Astronomy Technology Centre, Royal Observatory, Edinburgh, Blackford Hill, Edinburgh EH9 3HJ, UK*

<sup>3</sup>*Kapteyn Astronomical Institute, Postbus 800, 9700 AV Groningen, The Netherlands*

Accepted 2009. Received 2009 February 12

## ABSTRACT

The origin of Earth oceans is controversial. Earth could have acquired its water either from hydrated silicates (wet Earth scenario) or from comets (dry Earth scenario). [HDO]/[H<sub>2</sub>O] ratios are used to discriminate between the scenarios. High [HDO]/[H<sub>2</sub>O] ratios are found in Earth oceans. These high ratios are often attributed to the release of deuterium enriched cometary water ice, which was formed at low gas and dust temperatures. Observations do not show high [HDO]/[H<sub>2</sub>O] in interstellar ices. We investigate the possible formation of high [HDO]/[H<sub>2</sub>O] ratios in dense ( $n_{\text{H}} > 10^6 \text{ cm}^{-3}$ ) and warm gas ( $T = 100\text{--}1000 \text{ K}$ ) by gas-phase photochemistry in the absence of grain surface chemistry. We derive analytical solutions, taking into account the major neutral-neutral reactions for gases at  $T > 100 \text{ K}$ . The chemical network is dominated by photodissociation and neutral-neutral reactions. Despite the high gas temperature, deuterium fractionation occurs because of the difference in activation energy between deuteration enrichment and the back reactions. The analytical solutions were confirmed by the time-dependent chemical results in a  $10^{-3} M_{\odot}$  disc around a typical T Tauri star using the photochemical code PRODIMO. The PRODIMO code includes frequency-dependent 2D dust-continuum radiative transfer, detailed non-LTE gas heating and cooling, and hydrostatic calculation of the disc structure. Both analytical and time-dependent models predict high [HDO]/[H<sub>2</sub>O] ratios in the terrestrial planet forming region ( $< 3 \text{ AU}$ ) of circumstellar discs. Therefore the [HDO]/[H<sub>2</sub>O] ratio may not be a unique criterion to discriminate between the different origins of water on Earth.

**Key words:** Astrochemistry

## 1 INTRODUCTION

The water deuteration abundance ratio [HDO]/[H<sub>2</sub>O] is often used to determine the temperature at which water was synthesised. Current sub-millimeter observations already provide measurements of [HDO]/[H<sub>2</sub>O] for many astronomical objects including comets, hot-cores, and protoplanetary discs. In particular, a high [HDO]/[H<sub>2</sub>O] has been observed toward the protoplanetary disc DM Tau (Ceccarelli et al. 2005), although the HDO detection remains controversial (Guilloteau et al. 2006). The Herschel Space Telescope will be capable to detect cool and warm water in discs while the Atacama Large Millimeter Array (ALMA) will spatially resolve HDO emission.

The water deuteration abundance ratio [HDO]/[H<sub>2</sub>O] in hot cores around massive young stellar objects is  $\sim 3 \times 10^{-4}$  (Gensheimer et al. 1996), around a factor  $\sim 10$  enhancement compared to the cosmic [D]/[H] value set at the Big Bang ( $\sim 1.5 \times 10^{-5}$ , Linsky 2003). The enrichment suggests that the chemistry occurs in a low density, cold medium ( $T < 100 \text{ K}$ ), where HDO synthesis begins with the deuteration of the molecular ion H<sub>3</sub><sup>+</sup> into H<sub>2</sub>D<sup>+</sup> (e.g., Roberts & Millar 2000). Further gas-phase reactions lead to a high [HDO]/[H<sub>2</sub>O]. But at temperatures greater than 100 K, which is the typical gas temperature of hot cores, the initial deuteration reaction is inefficient and the [HDO]/[H<sub>2</sub>O] is

\* E-mail: wfdt@roe.ac.uk

† Scottish Universities Physics Alliances

close to the cosmic value. Therefore current chemical models need to invoke the evaporation of deuterium enriched water ice when the temperature reaches 100 K to explain the deuterium enrichment in water. The observed (HDO/H<sub>2</sub>O)<sub>ice</sub> ratio is however too low (Dartois et al. 2003; Parise et al. 2003). A second difficulty arises from the high observed water ice abundance of 10<sup>-5</sup>–10<sup>-4</sup>, which is two orders of magnitude larger than the gas phase abundance of water in the hot core around IRAS 16293-2422 (Parise et al. 2005).

After decades of research, the origin of water on Earth remains a major subject of debate (e.g., Nuth 2008 for a review). Two major models exist. In the first model, the Earth accretes dry: the building blocks of the Earth are made of dry rocks, composed only of silicates and carbonaceous materials. Most of the water is brought afterward by comets during the phase of heavy bombardment. This model is supported by the similarity between the Earth Mean Ocean Water (SMOW  $\simeq 1.49 \times 10^{-4}$ ) [HDO]/[H<sub>2</sub>O] and the cometary value, although the later value seems too high. Another support to the “dry” model is the low [HDO]/[H<sub>2</sub>O] predicted at temperature  $T > 100$  K by thermochemical equilibrium models. In the second model, most of the water on Earth comes from the release of water vapor trapped inside the water-entrapped planetesimals like carbonaceous chondrites upon impact or during volcanism. Water-rich planetesimals located at 2–3 AU are perturbed by the giant planets and collide with the young Earth (Morbidelli et al. 2000; Gomes et al. 2005; Raymond et al. 2004, 2005). Those planetesimals contain water in form of hydrated silicates. The average D/H in carbonaceous chondrite is similar to the value in the Earth ocean (Robert et al. 2000), although the composition of carbonaceous chondrite does not match the composition of Earth’s crust (Righter et al. 2006). The Earth is said to have accreted “wet” (Drake 2005). Hydrous material does not necessarily need to be brought from the asteroid belt area (2–3 AU). Recent study on adsorption of water molecules onto fractal dust grains shows that hydrous material could have been present in the vicinity of 1 AU (Stimpfl et al. 2006). In this scenario water in the gaseous solar nebula sticks onto the silicate surface of fractal grains, which coagulate and grow into the Earth. The adsorbed water would reflect the deuterium enrichment of the gas-phase water at 1 AU. The major difference between the two “wet” scenarios is that water was present in the early-Earth in the latter scenario. Geochemical findings suggest that hydrosphere and continental crust were already present in the first  $\sim 600$  million years of Earth history (Hopkins et al. 2008). The presence of water and also of organic matter at the formation of the Earth has profound astrobiology implications for the origin of life.

One major weakness of the “wet” scenario is that the deuterium enrichment predicted by equilibrium chemistry is too low at temperatures greater than 100 K. However there are chemical routes to obtain high [HDO]/[H<sub>2</sub>O] ratios at temperatures greater than 100 K in non-equilibrium chemistry. Photodissociation of H<sub>2</sub>O and HDO followed by reformation at the surface of protoplanetary discs and turbulent mixing can also change the [HDO]/[H<sub>2</sub>O] (Yung et al. 1988). Vertical turbulent mixing was invoked by Lyons & Young (2005) to explain the oxygen anomalies in the early solar nebula. Alternatively Genda & Ikoma (2008) propose that the [HDO]/[H<sub>2</sub>O] ratio on Earth changed during the evolution of the Earth from its formation. Willacy & Woods (2009) studied the deuterium chemistry of the inner disc around a T Tauri star and found relatively high HDO abundance in the warm molecular layer.

Four direct physical processes lead to isotopic fractionation in the gas phase. First, heavier isotopologues diffuse slower than the lighter main isotopologue. The diffusion results in zones of varying [HDO]/[H<sub>2</sub>O] ratios. This process is negligible in turbulent media when the mixing timescale is much lower than the diffusion timescales. Second, due to their larger reduced mass, isotopologues usually have a lower zero point energy. The vibrational energy levels are located lower, which increases the density sum of energy and hence reduces the vapor pressure. Hence, the water ice/gas ratios in the interstellar medium is not at equilibrium. Third, heavier isotopologues are chemically more stable because the binding energy between O and D is stronger than between O and H in the water molecule. Fractionation reactions dominate at low temperature because the inverse reactions have a minimum energy barrier equal to the difference in binding energy. Finally, isotopologues differ in their photodissociation cross section due to changes in the selection rules. A combination of the last two processes together with chemical diffusion and turbulent mixing probably determine the deuterium fractionation in the inner region of protoplanetary discs where terrestrial planets form.

Interstellar chemical models often neglect or include only few neutral-neutral reactions because their rates are small at temperatures below  $\sim 100$  K but they become competitively fast with the ion-neutral reactions at a few hundred degrees. For example, in dense and warm gases, the central species is the hydroxyl radical OH, which can react with H<sub>2</sub> to form H<sub>2</sub>O (Thi & Bik 2005).

In this paper, we explore neutral-neutral and photochemical reactions relevant to the formation and destruction of H<sub>2</sub>, HD, OH, OH, H<sub>2</sub>O and HDO at gas temperature between 100 and 1000 K. We first focus on steady-state abundances and perform an analytical analysis. Analytical analysis makes it possible to determine the main formation and destruction paths. After establishing the possible reaction paths, we use the photochemical code PRODIMO to compute a time-dependent chemical structure for a typical T Tauri disk to check the validity of our assumptions in the analytical analysis. In the rest of the paper, the chemical reaction rates are given in Table 4, 5, 6, 7, and 8. In particular, the most important reactions are summarised in Tables 4.

## 2 STEADY-STATE ANALYTICAL SOLUTION

### 2.1 Formation and destruction of H<sub>2</sub>O and HDO

We consider a gas mixture at a single temperature, density, irradiated by UV photons. In thermochemical equilibrium the deuterium exchange equilibrium reaction between water and molecular hydrogen (the most abundant reservoir of deuterium) is (e.g., Robert et al. 2000)



The equilibrium constant of this reaction for gas between 273 and 1000 K is (Richet et al. 1977)

$$K = \frac{P_{HDO}P_{H_2}}{P_{HD}P_{H_2O}} \simeq \frac{0.22 \times 10^6}{T^2} + 1. \quad (2)$$

The pressure dependence of  $K$  is negligible. At equilibrium, the deuterium enrichment decreases quadratically with temperature. A gas mixture is in thermochemical equilibrium when each chemical reaction is exactly balanced by its reverse reaction. Dissociations upon absorption of UV photons are not taken into account.

A gas is in chemical steady-state (also called stationary state) if the various abundances do not vary with time but the formation and destruction reactions for a given species are not necessarily the same. An analytical solution to the chemical network for the synthesis of H<sub>2</sub>O and HDO can be obtained by identifying the main formation and destruction chemical reactions. At high temperature ( $T > 100$  K) and density, it is well established that water is primarily formed via the reactions between the hydroxyl radical OH and molecular hydrogen H<sub>2</sub> (e.g, Thi & Bik 2005; Glassgold et al. 2009). High temperature gases are needed to overcome the large energy barrier of the reaction (reaction 5 with rate  $k_5$ ,  $E_a=1660$  K). The main destruction mechanism is likely photodissociation in low A<sub>V</sub> regions. Other water destruction mechanisms are reactions with atomic hydrogen, and with ionised helium in shielded regions. We assume in this study that the dust temperature  $T_d$  has equilibrated with the gas temperature. At  $T_d > 100$  K most water molecules remain in the gas phase. The rate of water formation is thus:

$$\frac{d[H_2O]}{dt} = (k_5[H_2] + k_{18}[HD] + k_7[OH])[OH] - (J_6 + k_8[H] + k_{19}[D] + k_{41}[He^+] + k_{cp,3})[H_2O], \quad (3)$$

where  $k_5$ ,  $k_{18}$ , and  $k_7$  are the rates of formation of water via the reactions OH+H<sub>2</sub>, OH+HD, and OH+OH respectively,  $J_6$  is the photodissociation rate,  $k_8$  is the water destruction rate by H,  $k_{cp,3}$  is the cosmic-ray induced photodissociation of water, and  $k_{41}$  is the rate of destruction by He<sup>+</sup>. At steady-state ( $d[H_2O]/dt = 0$ ), we obtain the ratio

$$\frac{[H_2O]}{[OH]} \simeq \frac{k_5[H_2]}{J_6 + k_8[H] + k_{41}[He^+] + k_{cp,3}}, \quad (4)$$

which will be used later in this paper. We have neglected the formation of water via reaction of OH with HD and OH and destruction of water via atomic deuterium because the rates are orders of magnitude smaller than the rates of other paths. Deuterated water can be formed via the reaction of HD with OH as well as via OD + H<sub>2</sub> (Bergin et al. 1998). Destruction occurs via photodissociation, reaction with atomic hydrogen and ionised helium.

$$\frac{d[HDO]}{dt} = k_{22}[OD][H_2] + k_{20}[OH][HD] - (J_{7a} + J_{7b} + (k_{21} + k_{23})[H] + (k_{42} + k_{43})[He^+] + k_{cp,4} + k_{cp,5})[HDO]. \quad (5)$$

The photodissociation of HDO can either lead to OH + D ( $J_{7a}$ ) or to OD + H ( $J_{7b}$ ). The sum of the two photorates is the total HDO photodissociation rate and is similar to the H<sub>2</sub>O photodissociation rate  $J_6$ . The photodissociation of HDO favors cleavage of the O-H bond over O-D bond with a 3 to 1 ratio (Shafer et al. 1989; Vander Wal et al. 1990, 1991), i.e.  $J_{7b} \simeq 3J_{7a}$  because the binding energy between O and D is stronger than that between O and H in water. In steady-state, the balance between formation and destruction leads to the ratio

$$X_D = \frac{[HDO]}{[H_2O]} = \frac{(k_{22}[OD][H_2] + k_{20}[OH][HD]) / (J_{7a} + J_{7b} + (k_{21} + k_{23})[H] + (k_{42} + k_{43})[He^+] + k_{cp,4} + k_{cp,5})}{k_5[OH][H_2] / (J_6 + k_8[H] + k_{41}[He^+] + k_{cp,3})}, \quad (6)$$

$$X_D = \frac{[HDO]}{[H_2O]} = \left( \frac{D_{H_2O}}{D_{HDO}} \right) \left( \frac{k_{22}([OD]/[OH])[H_2] + k_{20}[HD]}{k_5[H_2]} \right), \quad (7)$$

where we define

$$D_{H_2O} = J_6 + k_8[H] + k_{41}[He^+] + k_{cp,3} \quad (8)$$

and

$$D_{HDO} = J_{7a} + J_{7b} + (k_{21} + k_{23})[H] + (k_{42} + k_{43})[He^+] + k_{cp,4} + k_{cp,5} \quad (9)$$

to be the total destruction rates of H<sub>2</sub>O and HDO. The total UV photodissociation rates of H<sub>2</sub>O and HDO are similar (Zhang & Imre 1988):  $J_6 \simeq J_{7a} + J_{7b}$ . We further assume that rates with the deuterated species are similar to that of the main isotopologues:  $k_8 = k_{21} + k_{23}$ ,  $k_{41} \simeq k_{42} + k_{43}$ , and  $k_{cp,4} + k_{cp,5} = k_{cp,3}$ . If we can make the assumption that the total destruction rate of H<sub>2</sub>O and HDO are similar, i.e.  $D_{H_2O} \simeq D_{HDO}$ , then the value of [HDO]/[H<sub>2</sub>O] does not depend on the actual destruction mechanisms for H<sub>2</sub>O and HDO. The water fractionation  $f(\text{HDO})$  is defined as

$$f(\text{HDO}) = \frac{[HDO]/[H_2O]}{[HD]/[H_2]} = \left( \frac{D_{H_2O}}{D_{HDO}} \right) \left( \frac{k_{22}}{k_5} \frac{[OD]/[OH]}{[HD]/[H_2]} + \frac{k_{20}}{k_5} \right) = \left( \frac{D_{H_2O}}{D_{HDO}} \right) \left( \frac{k_{22}}{k_5} f(OD) + \frac{k_{20}}{k_5} \right) \simeq \frac{k_{22}}{k_5} f(OD) + \frac{k_{20}}{k_5} \quad (10)$$

The ratio  $k_{20}/k_5$  is the ratio between the reaction of OH with HD to form HDO compared to the reaction of OH with H<sub>2</sub> to form water. From the values in Table 4 the  $k_{20}/k_5$  ratio is lower than 1 for gas temperature greater than 120 K. This term does not enhance the water deuteration fractionation. We can write analytically the ratio between rate  $k_{22}$  and rate  $k_5$ :

$$\frac{k_{22}}{k_5} = \frac{1.55 \times 10^{-12} (T/300)^{1.6} e^{-1663/T}}{2.05 \times 10^{-12} (T/300)^{1.52} e^{-1660/T}} = 0.756098 (T/300)^{0.08} e^{-3/T}. \quad (11)$$

The ratio is weakly temperature-dependant. Since  $k_{22}/k_5 = 0.7 - 1$  between 100 and 1000 K, water and hydroxyl radical deuterium fraction are similar at gas temperature greater than  $\sim 200$  K:  $f(\text{HDO}) \simeq f(\text{OD})$ . Therefore water would be deuterium fractionated if OH is (i.e.  $f(\text{OD}) > 1$ ).

## 2.2 Formation and destruction of OH and OD

The water deuteration fraction  $f(\text{HDO})$  is intimately linked to that OH  $f(\text{OD})$ . The rate limiting reaction for the formation of water is the formation of hydroxyl radical OH:  $\text{O} + \text{H}_2 \rightarrow \text{OH} + \text{H}$  with rate  $k_1$ . This reaction has a large energy barrier ( $E_a=3163$  K). The chemistry of OD (and OH) is described in details by Croswell & Dalgarno (1985) for reactions without barrier. The production of OD mostly occurs through the rapid exchange reaction



once OH is present in the gas (reaction 16 with rate from Yung et al. 1988). The forward reaction has no activation barrier but the reverse reaction (reaction 13) has a barrier of 810 K because OD is more stable than OH. Thus at  $T < 1000$  K, OD is favored. The role of OD for gas between 100 and 1000 K is similar to that of  $\text{H}_2\text{D}^+$  for gas at  $T < 100$  K for the deuterium enrichment. OD can also formed by the reaction



OD is destroyed by reaction with carbon ion



and by photodissociation (with rate  $J_5$ )



The steady-state abundance of OH and OD taking into account the most important formation and destruction reactions are

$$[\text{OH}] = \frac{k_1[\text{O}][\text{H}_2] + (J_6 + k_8[\text{H}] + k_{41}[\text{He}^+] + k_{cp,3})[\text{H}_2\text{O}] + k_{14}[\text{O}][\text{HD}] + k_{22}[\text{OD}][\text{H}_2] + k_{30}[\text{CO}][\text{H}] + (J_{7a} + k_{cp,5})[\text{HDO}]}{(k_{15} + k_{16})[\text{D}] + k_4[\text{H}] + k_5[\text{H}_2] + k_{44}[\text{He}^+] + k_6[\text{O}] + k_{26}[\text{OD}] + k_{28}[\text{CO}] + k_{29}[\text{C}] + k_{39}[\text{C}^+] + J_4 + k_{cp,1}} \quad (17)$$

$$[\text{OH}] \simeq \frac{k_1[\text{O}][\text{H}_2]}{k_4[\text{H}] + k_5[\text{H}_2] + k_{28}[\text{CO}] + J_4 + k_{cp,1} + k_{29}[\text{C}] + k_{39}[\text{C}^+]} \quad (18)$$

After some algebra, we obtain the ratio

$$\frac{[\text{OH}]}{[\text{O}]} \simeq \frac{k_1[\text{H}_2]}{J_4 + k_4[\text{H}] + k_{28}[\text{CO}] + k_{cp,1} + k_{29}[\text{C}] + k_{39}[\text{C}^+] + k_{44}[\text{He}^+] + k_{cp,1}}, \quad (19)$$

which would be useful later in the analysis. For the deuterated hydroxyl radical at steady-state:

$$[\text{OD}] = \frac{k_{16}[\text{OH}][\text{D}] + k_{12}[\text{O}][\text{HD}] + k_{23}[\text{HDO}][\text{H}] + k_{25}[\text{O}_2][\text{D}] + k_{27}[\text{HDO}][\text{O}] + k_{33}[\text{CO}][\text{D}] + (J_{7b} + k_{cp,4})[\text{HDO}]}{k_{17}[\text{H}] + k_{22}[\text{H}_2] + k_{45}[\text{He}^+] + k_{24}[\text{O}] + k_{26}[\text{OH}] + k_{31}[\text{CO}] + k_{32}[\text{C}] + k_{40}[\text{C}^+] + J_5 + k_{cp,2}}. \quad (20)$$

The rates are listed in Table 1 to 5. Neglecting the minor formation and destruction reactions (i.e. reactions with C and  $\text{C}^+$ ), we simplify the ratio:

$$\frac{[\text{OD}]}{[\text{OH}]} \simeq \frac{D_{OH}}{D_{OD}} \left( \frac{k_{16}[\text{OH}][\text{D}] + k_{12}[\text{O}][\text{HD}] + (J_{7b} + k_{23}[\text{H}] + k_{cp,4})[\text{HDO}]}{k_1[\text{O}][\text{H}_2] + (J_6 + k_8[\text{H}] + k_{cp,3})[\text{H}_2\text{O}]} \right), \quad (21)$$

where

$$\frac{D_{OH}}{D_{OD}} = \frac{(k_{15} + k_{16})[\text{D}] + k_4[\text{H}] + k_5[\text{H}_2] + k_{44}[\text{He}^+] + k_6[\text{O}] + k_{26}[\text{OD}] + k_{28}[\text{CO}] + k_{29}[\text{C}] + k_{39}[\text{C}^+] + J_4 + k_{cp,1}}{k_{17}[\text{H}] + k_{22}[\text{H}_2] + k_{45}[\text{He}^+] + k_{24}[\text{O}] + k_{26}[\text{OH}] + k_{31}[\text{CO}] + k_{32}[\text{C}] + k_{40}[\text{C}^+] + J_5 + k_{cp,2}} \quad (22)$$

is the ratio between the sum of all destruction rates of OH and that of OD. The photodissociation rate of OH (rate  $J_4$ ) and OD (rate  $J_5$ ) are close (van Dishoeck & Dalgarno 1984; van Dishoeck 1988; Croswell & Dalgarno 1985) ( $J_4 \simeq J_5$ ). From Table 4 reactions 5 and 22 have similar rates ( $k_5 \simeq k_{22}$ ). Reactions 52 and 53 are ion-molecule reactions and we expect the rates to be of the same order of magnitude. Only reactions 4 ( $\text{OH} + \text{H} \rightarrow \text{O} + \text{H}_2$ ) and 17 ( $\text{OD} + \text{H} \rightarrow \text{OH} + \text{D}$ ) have very different rates, reaction 17 being much faster. But those reactions are important at low  $A_V$  only where photodissociation dominates as destruction process. We assume that  $k_6 \simeq k_{24}$ .

The hydroxyl radical deuterium fractionation reads

$$f(\text{OD}) = \frac{[\text{OD}]/[\text{OH}]}{[\text{HD}]/[\text{H}_2]} = \frac{D_{OH}}{D_{OD}} \left( \frac{k_{16}([\text{OH}]/[\text{O}])[\text{D}] + k_{12}[\text{HD}] + (J_{7b} + k_{23}[\text{H}] + k_{cp,4})X_D([\text{H}_2\text{O}]/[\text{O}])}{k_1[\text{H}_2] + (J_6 + k_8[\text{H}] + k_{cp,3})([\text{H}_2\text{O}]/[\text{O}])} \right) / \left( \frac{[\text{HD}]}{[\text{H}_2]} \right). \quad (23)$$

The OD fractionation increases with larger amount of OH and atomic deuterium and decreases if oxygen is in the atomic form and deuterium is locked in HD. Large amount of OH allows the deuterium exchange reaction to occur.

The knowledge of the abundances of H,  $\text{H}_2$ , D, and HD is needed to estimate the hydroxyl deuterium fraction  $f(\text{OD})$ .

### 2.3 H and H<sub>2</sub>

The formation of H<sub>2</sub> occurs mostly on grain surface when the grain temperature is below 1000 K and the destruction is caused by photodissociation at low A<sub>V</sub> and cosmic-ray/X-ray induced ionization and reaction with He<sup>+</sup> in the UV free region. The temperature is low enough to avoid H<sub>2</sub> destruction by atomic hydrogen. The steady-state balance between formation and destruction is:

$$R_1(T_g, T_d)n_H[H] = (f_{ss}J_1 + k_{\zeta,4} + k_{35}[He^+])[H_2], \quad (24)$$

where  $f_{ss}$  is the H<sub>2</sub> self-shielding function (Draine & Bertoldi 1996) and  $R_1(T_g, T_d)$  the molecular hydrogen formation rate on grain surfaces (Tielens 2005)

$$R_1(T_g, T_d) = 4.4 \times 10^{-17} S(T_g, T_d) \left( \frac{T_g}{100} \right)^{1/2}, \quad (25)$$

where  $T_g$  and  $T_d$  are the gas and dust grain temperature respectively and the sticking coefficient  $S$  is defined as

$$S(T_g, T_d) = \frac{1}{1 + 4 \times 10^{-2}(T_g + T_d)^{1/2} + 2 \times 10^{-3}T_g + 8 \times 10^{-6}T_g^2}. \quad (26)$$

The sticking coefficient ensures that at high dust temperature atomic hydrogen does not stick onto grain surfaces. The number density of nuclei is

$$n_H = [H] + 2[H_2] \quad (27)$$

We obtain the atomic and molecular abundances:

$$[H] = n_H \left( \frac{f_{ss}J_1 + k_{\zeta,4} + k_{35}[He^+]}{2R_1n_H + f_{ss}J_1 + k_{\zeta,4} + k_{35}[He^+]} \right) \simeq n_H \left( \frac{f_{ss}J_1 + k_{\zeta,4}}{2R_1n_H + f_{ss}J_1 + k_{\zeta,4}} \right) \quad (28)$$

and

$$[H_2] = n_H \left( \frac{R_1n_H}{2R_1n_H + f_{ss}J_1 + k_{\zeta,4} + k_{35}[He^+]} \right) \simeq n_H \left( \frac{R_1n_H}{2R_1n_H + f_{ss}J_1 + k_{\zeta,4}} \right). \quad (29)$$

Atomic and molecular hydrogen abundances are determined by the gas temperature, density, UV flux, extinction, the self-shielding function, and cosmic ray flux.

### 2.4 D and HD

While H<sub>2</sub> is predominately formed on grain surfaces, formation of HD can also occur in the gas phase by reaction between D and H<sub>2</sub> at high temperature and at density higher than about  $5 \times 10^3 \text{ cm}^{-3}$  (Le Petit et al. 2002). HD is destroyed by photodissociation and reaction with atomic H while H<sub>2</sub> is mainly photodissociated. H<sub>2</sub> can self-shield against photodissociation, HD is shielded by dust only. Therefore deuterium remains atomic at higher extinction than H<sub>2</sub>. In hot and dense regions, an important formation route of HD is therefore: H<sub>2</sub> + D → HD + H (reaction 10 with a barrier  $E_a=3820$  K). Larger amount of atomic deuterium is needed to obtain high OD over OH ratio. The production of atomic deuterium is enhanced at high temperature via the conversion reaction HD + H → H<sub>2</sub> + D. Another destruction mechanism of HD molecules involves photodissociation: HD + hν → H + D. Finally, reaction with H exchanges the atomic hydrogen with atomic deuterium: HD + H → H<sub>2</sub> + D. At high A<sub>V</sub>, cosmic rays destroy HD. Reactions with H<sup>+</sup> and atomic oxygen also destroy HD. The steady-state balance for [HD] then reads

$$[HD] = \frac{(k_{10}[H_2] + R_2n_H)[D] + k_{37}[D^+][H_2]}{J_2 + k_{\zeta,5} + k_{\zeta,6} + k_{11}[H] + k_{36}[H^+] + (k_{12} + k_{14})[O] + k_{18}[OH]}, \quad (30)$$

where  $R_2$  is the formation rate on grain surfaces (Le Petit et al. 2002) density

$$R_2(T_g, T_d) = 6.3 \times 10^{-17} S(T_g, T_d) \left( \frac{T_g}{100} \right)^{1/2} \quad (31)$$

and  $n_H$  is the total number. This H<sub>2</sub> formation rate does not take into account grain chemisorption sites contrary to more sophisticated H<sub>2</sub> formation model (Cazaux & Tielens 2002). We assume  $k_{\zeta,5} + k_{\zeta,6} \simeq k_{\zeta,4}$  and that the sticking coefficient is the same than for H<sub>2</sub>.

We neglect the formation of HD via reaction with D<sup>+</sup> and destruction via reactions with the protons, atomic oxygen and OH radicals. The steady-state balance leads to

$$\frac{[D]}{[HD]} = \frac{J_2 + k_{\zeta,4} + k_{11}[H]}{k_{10}[H_2] + R_2n_H} \quad (32)$$

If we can assume that most of the deuterium is locked in H and HD

$$n_D \simeq [D] + [HD], \quad (33)$$

then we obtain HD and D abundances

$$[HD] = n_D \left( \frac{k_{10}[H_2] + R_2 n_H}{J_2 + k_{\zeta,4} + k_{11}[H] + k_{10}[H_2] + R_2 n_H} \right) \quad (34)$$

and

$$[D] = n_D \left( \frac{J_2 + k_{\zeta,4} + k_{11}[H]}{J_2 + k_{\zeta,4} + k_{11}[H] + k_{10}[H_2] + R_2 n_H} \right). \quad (35)$$

At low  $A_V$ , destruction of [HD] is dominated by photodissociation and at gas temperature a few 100 K, the formation of HD via reaction of atomic deuterium with molecular hydrogen is negligible

$$\frac{[D]}{[HD]} \simeq \frac{J_2}{R_2 n_H}. \quad (36)$$

Even in obscured ( $J_2 \sim 0$ ) and fully molecular regions ( $[H] \sim 0$ ), cosmic-rays induced photodissociation and deuterium exchange reactions ensure that some atomic deuterium always remains in atomic form:

$$\frac{[D]}{[HD]} \simeq \frac{k_{\zeta,4}}{R_2 n_H}. \quad (37)$$

The formation of HD on grains decreases dramatically for dust grain temperature above 100 K.

## 2.5 Neutral and ionised Helium

Where the steady-state abundance of ionised Helium is given by the expression:

$$[He^+] = \frac{k_{\zeta,3}[He]}{k_{35}[H_2] + k_{e-,3}[e^-]} \quad (38)$$

Combining with the element conservation equation:

$$n_{He} = [He] + [He^+] \quad (39)$$

we obtain

$$[He^+] = \frac{k_{\zeta,3} n_{He}}{k_{35}[H_2] + k_{e-,3}[e^-] - k_{\zeta,3}} \quad (40)$$

The  $He^+$  abundance can be estimated only if the electron abundance is known. Our simple analytical analysis cannot provide an estimate of the  $He^+$  abundance and we will omit in the rest of the paper reactions with  $He^+$ .

## 2.6 Water fractionation ratio $f(HDO)$

The results of the previous sections can be combined to derive an analytical formula of the [HDO]/[H<sub>2</sub>O] ratio:

$$X_D = \frac{[HDO]}{[H_2O]} = num/den, \quad (41)$$

where

$$num = \frac{k_{22}}{k_5} \left( \frac{D_{OH}}{D_{OD}} \frac{D_{H_2O}}{D_{HD O}} \right) \frac{k_{16}([OH]/[O])[D] + k_{12}[HD]}{k_1[H_2] + (J_6 + k_8[H] + k_{cp,3})([H_2O]/[O])} + \frac{k_{20}}{k_5} \frac{[HD]}{[H_2]} \quad (42)$$

and

$$den = 1 - \frac{k_{22}}{k_5} \left( \frac{D_{OH}}{D_{OD}} \frac{D_{H_2O}}{D_{HD O}} \right) \frac{(J_{7b} + k_{23}[H] + k_{cp,4})([H_2O]/[O])}{k_1[H_2] + (J_6 + k_8[H] + k_{cp,3})([H_2O]/[O])} \quad (43)$$

The abundances and abundance ratios in *num* and *den* have been derived earlier:

$$\frac{[OH]}{[O]} \simeq \frac{k_1[H_2]}{J_4 + k_4[H] + k_{28}[CO] + k_{29}[C] + k_{39}[C^+] + k_{44}[He^+] + k_{cp,1}}, \quad (44)$$

$$\frac{[H_2O]}{[OH]} = \frac{k_5[H_2]}{J_6 + k_8[H] + k_{41}[He^+] + k_{cp,3}}, \quad (45)$$

and combining the two equations above, we obtain

$$\frac{[H_2O]}{[O]} = \frac{k_1 k_5 [H_2]^2}{(J_4 + k_4[H] + k_{28}[CO] + k_{29}[C] + k_{39}[C^+] + k_{44}[He^+] + k_{cp,1})(J_6 + k_8[H] + k_{41}[He^+] + k_{cp,3})}. \quad (46)$$

The water fractionation is composed of 3 terms. At gas temperature greater than 200 K the second term  $k_{12}/k_1$  dominates for both low and high extinction and the fractionation reaches 10-1000. Our analysis concerns high temperature gas only. In warm and dense region, the main

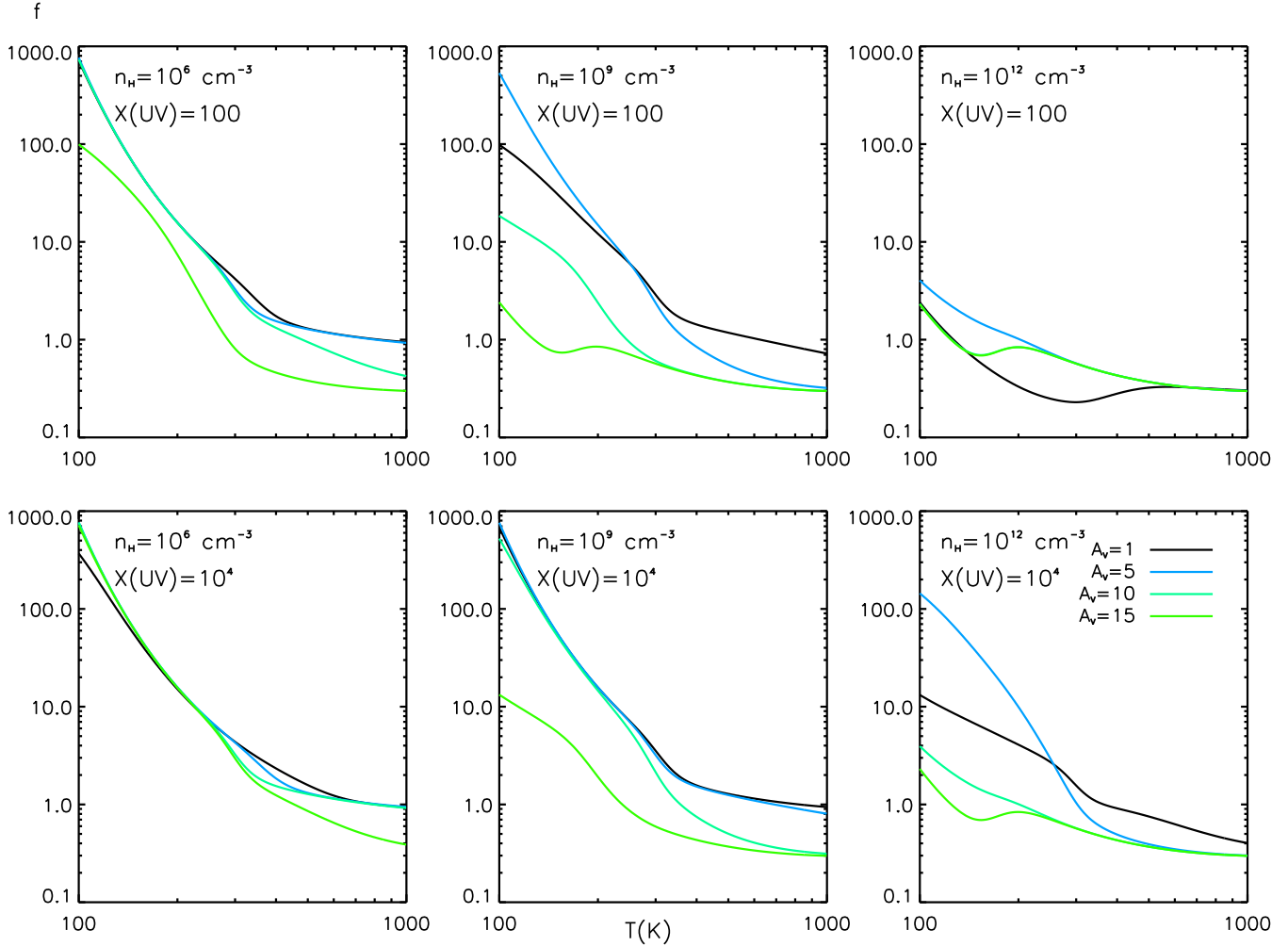


**Figure 1.** Water deuteration fraction  $f(\text{HDO})$ . The upper panels show models with UV enhancement of factor 100 w.r.t. the standard interstellar UV field and for three increasing gas densities. The four curves correspond to the various dust extinctions. The lower panels are models with UV enhancement of  $10^4$ .

oxygen carrier is water and that of carbon is methane CH<sub>4</sub> and not CO at high  $A_V$  and C<sup>+</sup> at low  $A_V$ . As state before, we further neglect reactions with He<sup>+</sup>.

At temperature below 100 K, the only fast chemical reactions are between ions and neutral species, which are not taken into account in our analysis. The starting point of water formation is H<sub>3</sub><sup>+</sup>. Deuterium enrichment occurs via the deuterated equivalent of H<sub>3</sub><sup>+</sup>, H<sub>2</sub>D<sup>+</sup>. H<sub>2</sub>D<sup>+</sup> has a lower zero-point energy, which favors the deuteration reaction H<sub>3</sub><sup>+</sup> + HD → H<sub>2</sub>D<sup>+</sup> + H<sub>2</sub>. The rate of the back reaction has an energy barrier of 230 K.

The water deuteration fraction enhancement is caused by the fast deuterium exchange reaction with OH (D+OH → OD + H). The inverse reaction has an energy barrier of 717 K. Significant amount of atomic deuterium is possible at low and intermediate extinction. We plotted in Fig. 1 the ratio [HDO]/[H<sub>2</sub>O] as function of the gas temperature for an impinging UV enhanced by a factor  $10^4$  and  $10^2$ , for different extinctions ( $A_V=1, 5, 10, 15$ ), and for two gas densities ( $n_H = 10^8$  and  $10^{12}$  cm<sup>-3</sup>). Disc surfaces around young accreting T Tauri stars receive  $\sim 10^4$  to  $10^6$  times the amount of standard interstellar UV. The UV field, extinction, density, and gas temperature values are typically found in regions of discs where water is abundant. In the following section, we will use a time-dependent thermo-photochemical code to support our assumed values for the parameters. The figure shows that large  $f(\text{HDO})=[\text{HDO}]/[\text{H}_2\text{O}]$  ratios (up to a few 100) are possible for gas temperatures up to 500-600 K and up to extinction of 10, although the average value for  $f$  is lower than 10. At  $T > 500$ , the back reaction OD+H → OH+D starts to destroy efficiently OD. The figure also shows the large range of values for  $f(\text{HDO})$  (0.1– $10^3$ ). The  $f(\text{HDO})$  curves testify of the sensitivity of the abundances on the gas temperature, which reflects the exponential nature of the Arrhenius' law for neutral-neutral reactions.

**Table 1.** Stellar and disc parameters

Stellar mass	$M_*$	$0.8 M_\odot$
Stellar luminosity	$L_*$	$0.7 L_\odot$
Effective temperature	$T_{\text{eff}}$	4400 K
Disc mass	$M_d$	$10^{-3} M_\odot$
Disc inner radius	$R_{\text{in}}$	0.1 AU
Disc outer radius	$R_{\text{out}}$	300 AU
Vertical column density power law index	$\epsilon$	1
dust to gas mass ratio		0.01
dust grain material mass density	$\rho_{\text{dust}}$	$2.5 \text{ g cm}^{-3}$
minimum dust particle size	$a_{\text{min}}$	$0.01 \mu\text{m}$
maximum dust particle size	$a_{\text{max}}$	$100 \mu\text{m}$
dust size distribution power law	$p$	3.5
Cosmic ray flux	$CR$	$1.7 \times 10^{-17} \text{ s}^{-1}$
ISM UV field w.r.t. Draine field	$\chi$	1.0
abundance of PAHs relative to ISM	$f_{\text{PAH}}$	0.1
$\alpha$ viscosity parameter	$\alpha$	0.0

### 3 TIME-DEPENDENT MODELLING

#### 3.1 PRODIMO photochemical code

We modelled the chemical abundances of a  $10^{-3} M_\odot$  disc around a typical T Tauri star ( $T_{\text{eff}} 4400 \text{ K}$ ,  $\log g=4.0$ ,  $Z=1.0$ ) using the photochemical code PRODIMO. PRODIMO combines frequency-dependent 2D dust-continuum radiative transfer, kinetic gas-phase and UV photochemistry, ice formation, and detailed non-LTE heating and cooling balance. The major improvement over previous studies is that the density structure is determined by the gas pressure that is computed by detailed chemistry and energy balanced and not by assuming that the gas and dust have the same temperature. Detailed description of the code are given by Woitke et al. (2009) and in Kamp et al. (2009). The code has been used to determine the water abundance in the inner disc around a typical Herbig Ae star (Woitke et al. 2009). The most recent additions to the code includes PAH chemistry, time-dependent chemistry, deuterium chemistry, and generation of Spectral Energy Distribution and spectral lines. The last two features are not used in the modelling performed for this paper. Table 1 summarized the input parameters to the model. The stellar spectrum was generated using PHOENIX (Brott & Hauschildt 2005) with the addition of chromospheric flux from HD 129333 (Dorren & Guinan 1994). Although the model extends to 300 AU, we focus here only on the inner 3 AU as we are interested in the  $[\text{HDO}]/[\text{H}_2\text{O}]$  ratio in the terrestrial planet forming region of discs.

The chemical network includes a total of 187 deuterated and non-deuterated gas and ice species. Most reaction rates are taken from the UMIST DATABASE (Woodall et al. 2007). Additional reaction rates were compiled from the NIST chemical kinetic database. The rates involving deuterated species are described in e.g., Roberts et al. (2004), Roberts & Millar (2000), Charnley et al. (1997), and Brown & Millar (1989). Species can freeze-out onto grain surfaces and desorb thermally or upon absorption of a cosmic-ray or a UV photon (photodesorption). Grain surface reactions were omitted apart from the grain surface formation of  $\text{H}_2$  and HD (Cazaux & Tielens 2002). The photodissociation cross-sections are taken from the LEIDEN DATABASE described in van Dishoeck et al. (2008).

The chemical abundances in the disc were established in three stages. First PRODIMO determined the UV field, hydrostatic density, gas and dust temperature, and chemical abundance structure self-consistently assuming steady-state chemistry. Second we computed the chemical abundances of gas and solid species for a 1 Myr old molecular cloud with density of  $5 \times 10^4 \text{ cm}^{-3}$  and gas and dust temperature of 15 K from diffuse cloud initial abundances, where the elements are in neutral or ionized atomic form (see Table 2). Third we ran PRODIMO in the time-dependent chemical mode to simulate the chemical structure of a 1 Myr old disc using the results of the molecular cloud run as initial chemical abundances and the disc properties computed in the first stage. All other disc properties (UV field, density and temperature structure) were fixed in this last stage.

The three-stage method mimics the incorporation of molecular cloud materials and their subsequent evolution in the disc. It also makes it possible to compare the chemical abundances obtained with the time-dependent model and at steady-state. Our approach differs from Visser et al. (2009) who solve the chemistry in a Lagrangian frame and their disc evolves according to viscous spreading. However their number of species and reactions are limited.

#### 3.2 Model results

Figure 2 show the UV field, density, and gas and dust temperature structure in the inner 3 AU. The disc structure is discussed in Woitke et al. (2009). In this paper we focus on the water and HDO abundances. Figure 3 show the water and HDO abundances at steady-state on the left and for a disc of 1 Myr old on the right. Apart from the  $\text{H}_2\text{O}$  HDO in the midplane beyond  $\sim 1.5\text{--}2 \text{ AU}$ , the water and HDO abundances



**Table 2.** Typical diffuse cloud abundances used as initial abundances for the molecular cloud chemical calculation. Species with ionization potential (IP) higher than 13.6 eV are neutral while species with IP below 13.6 eV are ionized. The other species have negligible initial abundance.

Species	$\log(n(X)/n_{\text{H}})$
H	0.0
D	-5.0
He	-1.125
C <sup>+</sup>	-3.886
O	-3.538
N	-4.67
S <sup>+</sup>	-5.721
Si <sup>+</sup>	-5.1
Mg <sup>+</sup>	-5.377
Fe <sup>+</sup>	-5.367
PAH	-6.52

**Table 3.** Mass and average gas and dust temperature for the three gas-phase water and HDO locations. The paper focuses mostly on the inner midplane.

Location	Mass (M <sub>⊙</sub> )	$\langle T_{\text{gas}} \rangle$ (K)	$\langle T_{\text{dust}} \rangle$ (K)
H <sub>2</sub> O			
Inner midplane	$2.6 \times 10^{-8}$	178	177
Cold belt	$1.1 \times 10^{-9}$	16	16
Hot layer	$2.1 \times 10^{-12}$	1147	120
HDO			
Inner midplane	$1.2 \times 10^{-10}$	140	140
Cold belt	$3.8 \times 10^{-11}$	16	16
Hot layer	$2.6 \times 10^{-14}$	474	102

are similar for the steady-state and time-dependent chemistry models. The differences stem from the fact that at steady-state even very slow reactions will impact the chemistry. In this case, the dust temperature is low enough ( $T_{\text{d}} < 150$  K) such that all water and HDO should be frozen-out. In the time-dependent model, significant amount of water and HDO remains in the gas-phase in the inner 1 AU or above the ice zone. The differences between the steady-state and time-dependent abundances occur in low gas-phase water abundance regions and thus do not impede our analysis of deuterium enrichment for gas-phase water either outside the water freeze-out zone.

The [HDO]/[H<sub>2</sub>O] ratio for the time-dependent model is plotted in Figure 4. The water abundance levels at  $10^{-6}$  and  $10^{-8}$  are overlaid. Water is abundant as soon as hydrogen is in molecular form. In our model, water and HDO are frozen onto grain surfaces in the midplane beyond  $\sim 1.5$  AU as shown in Figure. 5. The gas-phase [HDO]/[H<sub>2</sub>O] ratio decreases with radius. At 0.5–1.5 AU in the mid-plane, the ratio is a few  $10^{-3}$ – $10^{-2}$ . Gas-phase water and HDO are located in three zones: the inner midplane, the cold belt, and the hot layer (Woitke et al. 2009). The mass and average gas and dust temperature are given in Table 3.

Most of the gas-phase water ( $n(\text{H}_2\text{O})/n_{\text{H}}=10^{-8}$ – $10^{-5}$ ) is located in the inner plane close to the star ( $R < 1$  AU). In the inner 30 AU a small fraction is found above the mid-plane (Woitke et al. 2009), where the vertical extinction  $A_{\text{V}}$  is between 1 and 10. Although of insignificant mass, the molecules are hot and emit strongly (e.g. Carr & Najita 2008; Salyk et al. 2008). In the outer disc, gas-phase water is found in a cold belt, which is sandwiched between  $A_{\text{V}} \sim 1$  and 5 where efficient photodesorption maintains some water molecules in the gas phase (see (Woitke et al. 2009)). Since HDO and H<sub>2</sub>O have similar adsorption energy, the gas-phase abundance of both species are co-located (see Fig.3). We plotted the vertical column densities for H, D, OH, OD, H<sub>2</sub>O, HDO, H<sub>2</sub>O#, and HDO# in Fig. 6. This figure shows that the column density ratios HDO/H<sub>2</sub>O, HDO#/H<sub>2</sub>O#, and OD/OH stay relatively constant in the inner disc, with values much higher than the elemental D/H ratio of  $10^{-5}$ .

In the high water abundance region, the [HDO]/[H<sub>2</sub>O] ratio is higher than  $10^{-2}$ . Using the mass of H<sub>2</sub>O and HDO in the inner midplane listed in Table 3, we derived an average [HDO]/[H<sub>2</sub>O] ratio of  $4.6 \times 10^{-3}$ , which is 30 times higher than the Earth Mean Ocean Water value ( $\simeq 1.49 \times 10^{-4}$ ) and close to cometary values. The actual [HDO]/[H<sub>2</sub>O] values in our models depend on the disc parameters. Future studies with focus on the effect of disc properties (disc mass, radius, ...) on the [HDO]/[H<sub>2</sub>O] ratios.

Overall, the [HDO]/[H<sub>2</sub>O] ratios in the inner disc midplane by the time-dependent code PRODIMO are consistent with the analytical results. Our results contradict the simple decrease in [H<sub>2</sub>O]/[HDO] with increasing temperature if thermochemical equilibrium ratios are assumed.

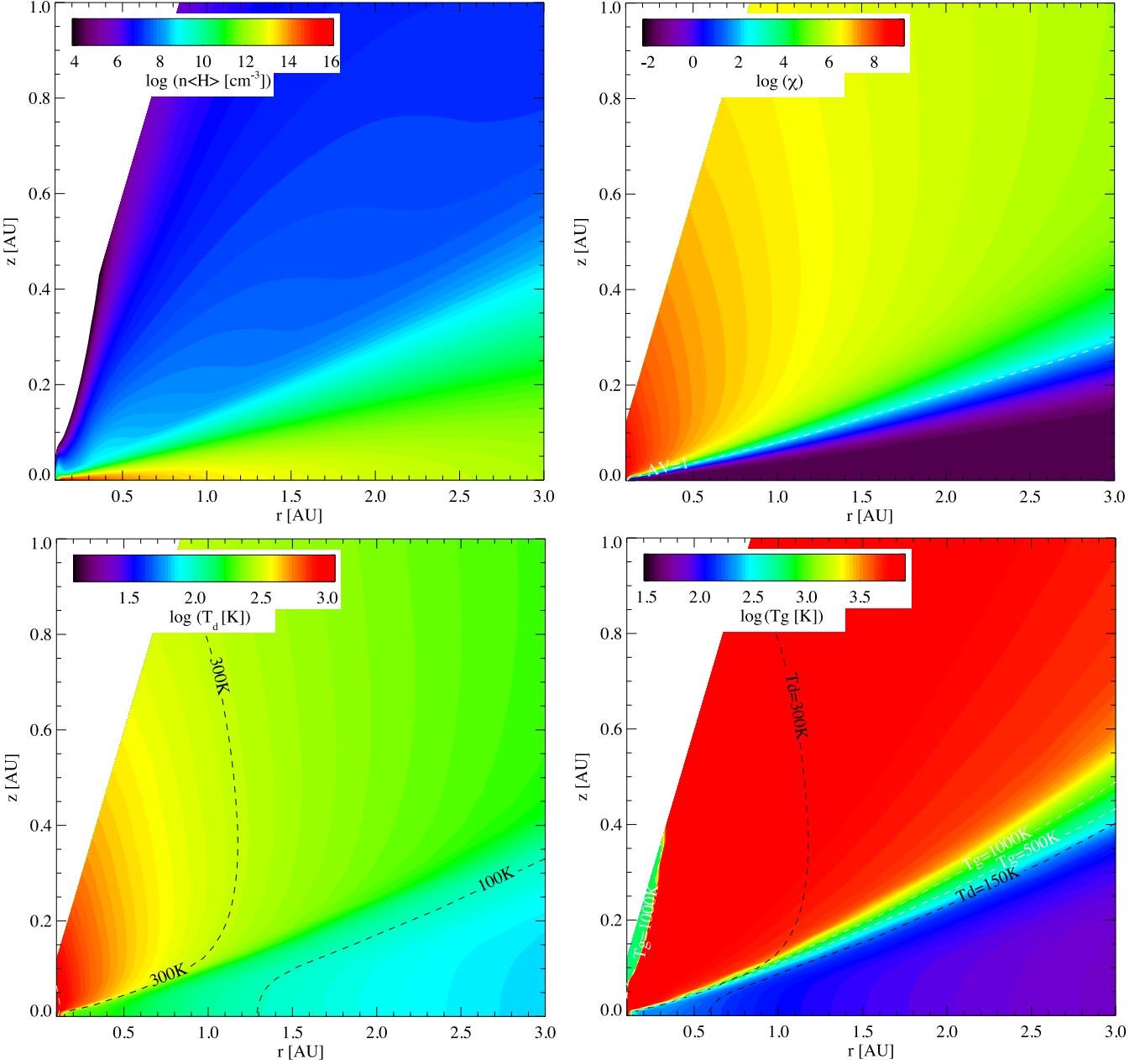


**Figure 2.** The four panels show the gas density  $n_{<H>}$  (upper left), strength of the UV field with respect to the Draine field  $\chi$  (upper right), the dust temperature  $T_d$  (lower left), and the gas temperature  $T_g$  with dust and gas temperature overlaid (lower right) for the inner 3 AU computed by PRODIMO. The structure is consistent with the chemical abundances.

#### 4 DISCUSSION AND CONCLUSION

A simple analytical analysis shows that high water fraction is possible in a simple deuteration chemical network for gas hotter than 100 Kelvin if neutral-neutral reactions are included. The analytical results are supported by the time-dependent photochemical model results. In their study Willacy & Woods (2009) also found that HDO can be abundant in the inner disc.

The water deuterium fractionation is determined by the ratio between the rate of formation of OD via  $\text{O} + \text{HD}$  and the rate of formation of OH via  $\text{O} + \text{H}_2$ . Lower zero-point energy for HD makes the first reaction faster than the second one above 200 K. At low temperature ( $T < 100$  K), fast deuteration of  $\text{H}_3^+$ , the main driver of cold gas-phase chemistry ensures that main molecules are deuterium-enriched. Another reason for higher HDO/ $\text{H}_2\text{O}$  is the preferential branching into  $\text{OD} + \text{H}$  when HDO is photodissociated (Shafer et al. 1989; Vander Wal et al. 1990, 1991).

From our work, it is also theoretically possible to have high water deuterium fractionation from gas-phase photo-chemistry above 200 K. Deuterium enrichment can also occur at high temperature because of the energy difference in activation barrier for deuterium exchange and the back reactions. Finally, water deuterium enrichment is not as stringent a constraint as thought for the origin of water on Earth. Deuterium-

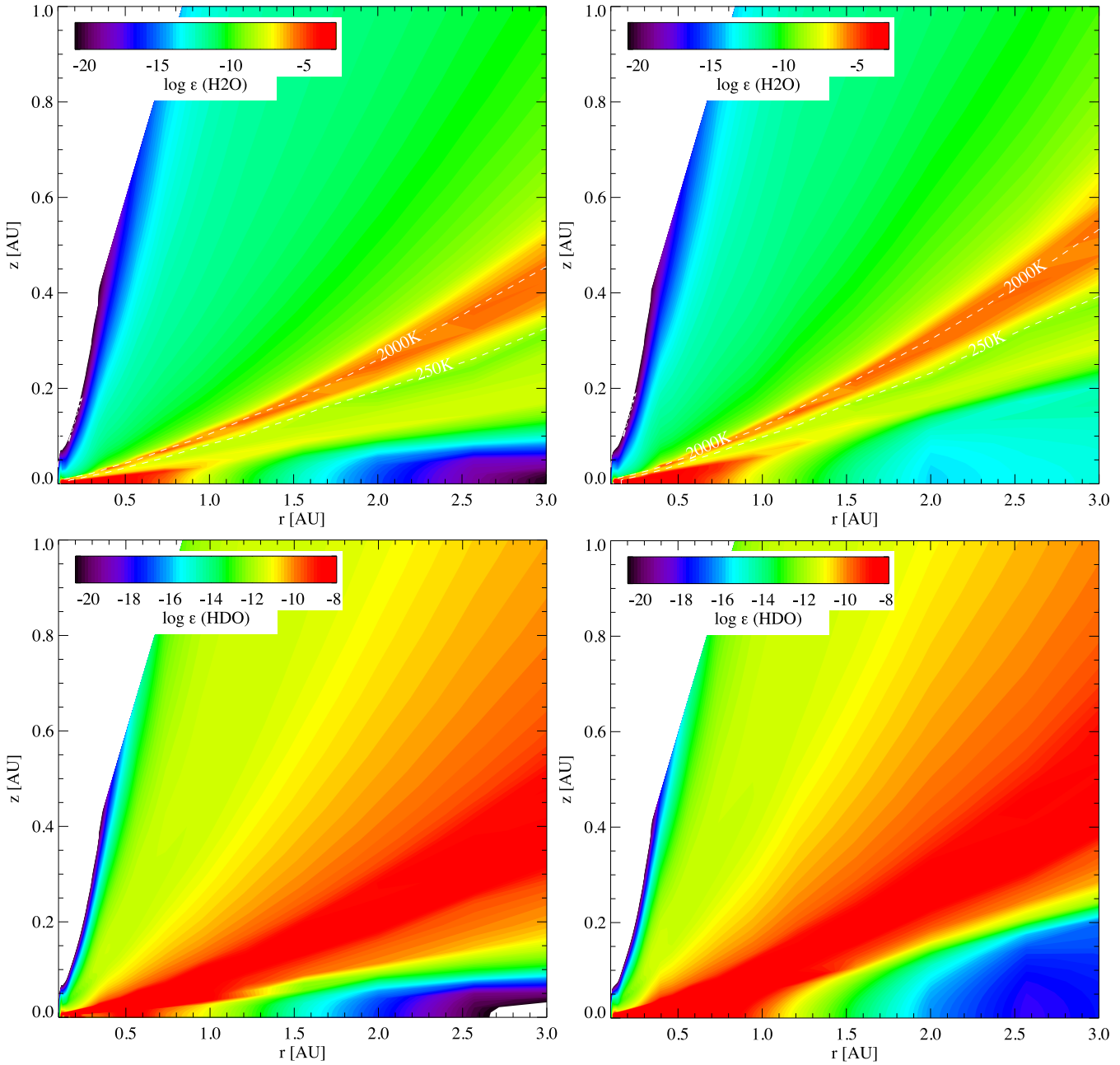


**Figure 3.** Gas-phase H<sub>2</sub>O and HDO abundance in the inner 3 AU computed by PRODIMO. The left panels show the steady-state abundances while the right panels show the time-dependent abundances for a 1 Myr old disc.

enriched water may have been synthesised at  $\sim 1$  AU and incorporated directly onto silicate dust grains (Stimpfl et al. 2006). Water could have been incorporated on Earth already at the stage of planetesimals accretion. However our simple analytical steady-state chemical model and the 2D modelling with PRODIMO do not include effects of turbulent mixing in protoplanetary discs, both radial and vertical.

## 5 ACKNOWLEDGMENTS

WFT is supported by a Scottish Universities Physics Alliance (SUPA) fellowship in Astrobiology. We thank the referee for his/her comments.

**Table 4.** Principal reactions

Reaction	A ( $\text{cm}^3 \text{s}^{-1}$ )	B	$E_a$ (K)	Reference
$k_1$ O + H <sub>2</sub> → OH + H	$3.14 \times 10^{-13}$	2.7	3150	UMIST
$k_5$ OH + H <sub>2</sub> → H <sub>2</sub> O + H	$2.05 \times 10^{-12}$	1.52	1660	UMIST
$k_{10}$ H <sub>2</sub> + D → HD + H	$7.50 \times 10^{-11}$	–	3820	Zhang & Millar 1989
$k_{11}$ HD + H → H <sub>2</sub> + D	$7.50 \times 10^{-11}$	–	4240	Zhang & Millar 1989
$k_{12}$ O + HD → OD + H	$1.57 \times 10^{-12}$	1.7	4639	Joseph, Truhlar & Garret 1988
$k_{16}$ OH + D → OD + H	$9.07 \times 10^{-11}$	-0.63	–	Yung et al. 1988
$k_{20}$ OH + HD → HDO + H	$0.60 \times 10^{-13}$	1.9	1258	Talukdar et al. 1996
$k_{22}$ OD + H <sub>2</sub> → HDO + H	$1.55 \times 10^{-12}$	1.6	1663	Talukdar et al. 1996

Reaction	q	$\gamma$ ( $\text{s}^{-1}$ )	Reference
$J_2$ HD + $h\nu$ → H + D	$2.6 \times 10^{-11}$	2.5	–
$J_4$ OH + $h\nu$ → O + H	$3.5 \times 10^{-10}$	1.7	–

Ref. UMIST: Woodall et al. (2007)

**Table 5.** Neutral-neutral and radical-neutral reactions

Reaction	A ( $\text{cm}^3 \text{s}^{-1}$ )	B (K)	$E_a$ (K)	Reference
$R_1$ H + H + M → H <sub>2</sub>	–	–	–	see text
$R_2$ H + D + M → HD	–	–	–	see text

$k_1$ O + H <sub>2</sub> → OH + H	$3.14 \times 10^{-13}$	2.70	3150	UMIST
$k_2$ O <sub>2</sub> + H → OH + H	$2.61 \times 10^{-10}$	–	8156	UMIST
$k_3$ O <sub>2</sub> + H <sub>2</sub> → OH + OH	$3.16 \times 10^{-10}$	–	21890	UMIST
$k_4$ OH + H → O + H <sub>2</sub>	$7.00 \times 10^{-14}$	2.80	1950	UMIST
$k_5$ OH + H <sub>2</sub> → H <sub>2</sub> O + H	$2.05 \times 10^{-12}$	1.52	1660	UMIST
$k_6$ OH + O → O <sub>2</sub> + H	$1.77 \times 10^{-11}$	–	-178	UMIST
$k_7$ OH + OH → O + H <sub>2</sub> O	$3.87 \times 10^{-13}$	1.69	-469	UMIST
$k_8$ H <sub>2</sub> O + H → OH + H <sub>2</sub>	$1.59 \times 10^{-11}$	1.20	9610	UMIST
$k_9$ H <sub>2</sub> O + O → OH + OH	$1.85 \times 10^{-11}$	0.95	8571	UMIST
$k_{10}$ H <sub>2</sub> + D → HD + H	$7.50 \times 10^{-11}$	–	3820	Zhang & Millar 1989
$k_{11}$ HD + H → H <sub>2</sub> + D	$7.50 \times 10^{-11}$	–	4240	Zhang & Millar 1989
$k_{12}$ O + HD → OD + H	$1.57 \times 10^{-12}$	1.7	4639	Joseph, Truhlar & Garret 1988
$k_{13}$ OD + H → O + HD	–	–	–	$k_{13} = k_4$ is assumed
$k_{14}$ O + HD → OH + D	$9.01 \times 10^{-13}$	1.9	3730	Joseph, Truhlar & Garret 1988
$k_{15}$ OH + D → O + HD	–	–	–	$k_{15} = k_4$ is assumed
$k_{16}$ OH + D → OD + H	$9.07 \times 10^{-11}$	-0.63	–	Yung et al. 1988
$k_{17}$ OD + H → OH + D	$1.26 \times 10^{-10}$	-0.63	717	Yung et al. 1988
$k_{18}$ OH + HD → H <sub>2</sub> O + D	$2.12 \times 10^{-13}$	2.7	1258	Talukdar et al. 1996
$k_{19}$ H <sub>2</sub> O + D → OH + HD	–	–	–	$k_{19} = k_8$ is assumed
$k_{20}$ OH + HD → HDO + H	$0.60 \times 10^{-13}$	1.9	1258	Talukdar et al. 1996
$k_{21}$ HDO + H → OH + HD	–	–	–	$k_{21} = 0.5 \times k_8$ is assumed
$k_{22}$ OD + H <sub>2</sub> → HDO + H	$1.55 \times 10^{-12}$	1.6	1663	Talukdar et al. 1996
$k_{23}$ HDO + H → OD + H <sub>2</sub>	–	–	–	$k_{23} = 0.5 \times k_8$ is assumed
$k_{24}$ OD + O → O <sub>2</sub> + D	–	–	–	$k_{24} = k_6$ is assumed
$k_{25}$ O <sub>2</sub> + D → OD + O	–	–	–	$k_{25} = k_2$ is assumed
$k_{26}$ OD + OH → O + HDO	–	–	–	$k_{26} = k_7$ is assumed
$k_{27}$ HDO + O → OD + OH	–	–	–	$k_{27} = k_9$ is assumed

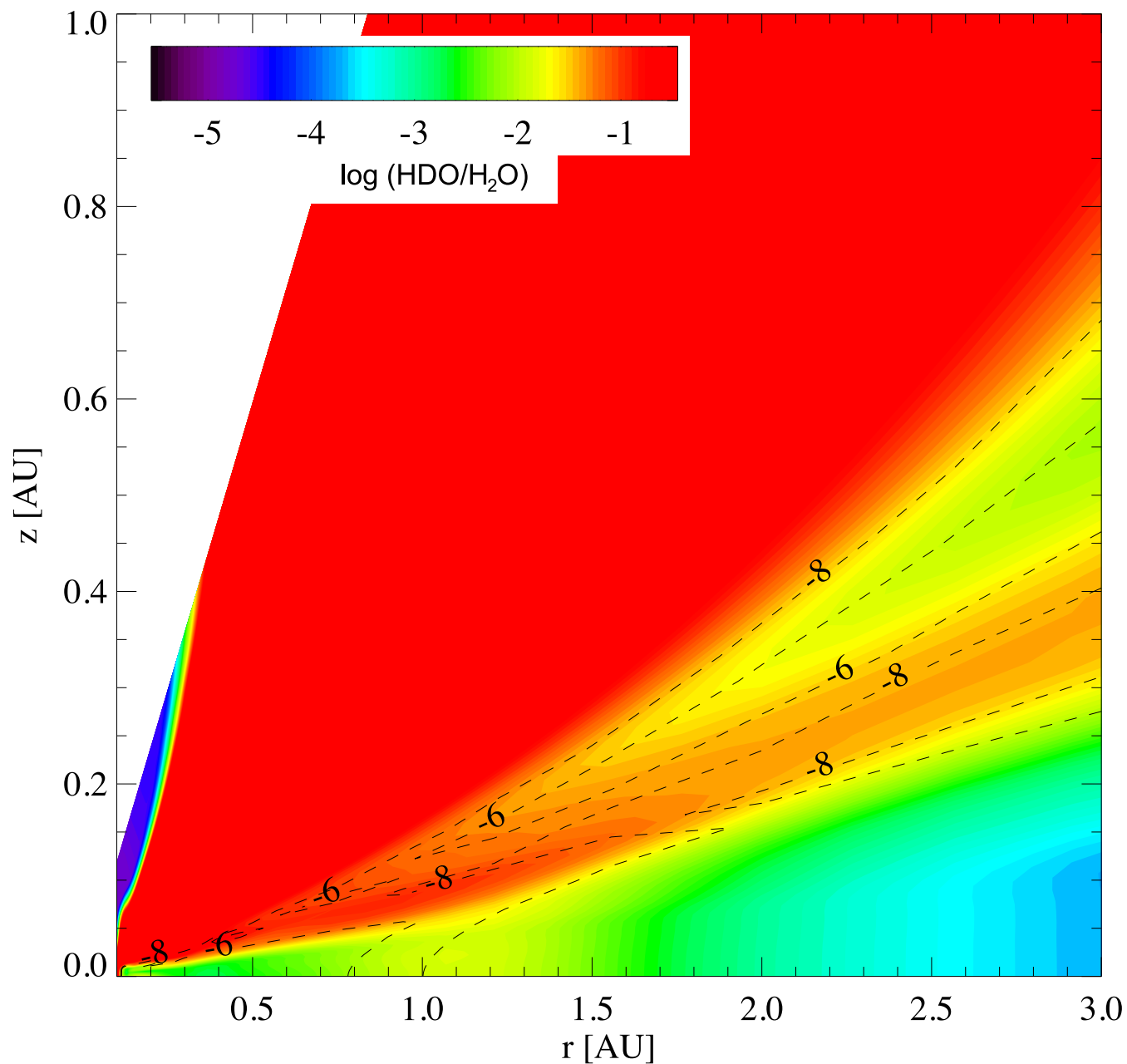
  

$k_{28}$ OH + CO → CO <sub>2</sub> + H	$1.17 \times 10^{-13}$	0.95	-74.0	UMIST
$k_{29}$ OH + C → CO + H	$1.10 \times 10^{-10}$	0.5	0.0	UMIST
$k_{30}$ CO + H → OH + C	$1.10 \times 10^{-10}$	0.5	77700.0	UMIST

$k_{31}$ OD + CO → CO <sub>2</sub> + D	–	–	–	$k_{31} = k_{28}$ is assumed
$k_{32}$ OD + C → CO + D	–	–	–	$k_{32} = k_{29}$ is assumed
$k_{33}$ CO + D → OD + C	–	–	–	$k_{33} = k_{30}$ is assumed

Ref. UMIST: Woodall et al. (2007)



**Figure 4.**  $[\text{HDO}]/[\text{H}_2\text{O}]$  in the 3 AU of a  $10^{-3}$  disc as computed by the photochemical code PRODIMO. The contours indicate the regions where gas-phase water abundance is  $10^{-6}$  and  $10^{-8}$ .

## REFERENCES

- Bergin E. A., Neufeld D. A., Melnick G. J., 1998, *ApJ*, 499, 777  
 Brott I., Hauschildt P. H., 2005, in C. Turon, K. S. O’Flaherty, & M. A. C. Perryman ed., *The Three-Dimensional Universe with Gaia* Vol. 576 of ESA Special Publication, A PHOENIX Model Atmosphere Grid for Gaia. pp 565–+  
 Brown P. D., Millar T. J., 1989, *MNRAS*, 237, 661  
 Carr J. S., Najita J. R., 2008, *Science*, 319, 1504  
 Cazaux S., Tielens A. G. G. M., 2002, *ApJL*, 575, L29  
 Ceccarelli C., Dominik C., Caux E., Lefloch B., Caselli P., 2005, *ApJL*, 631, L81

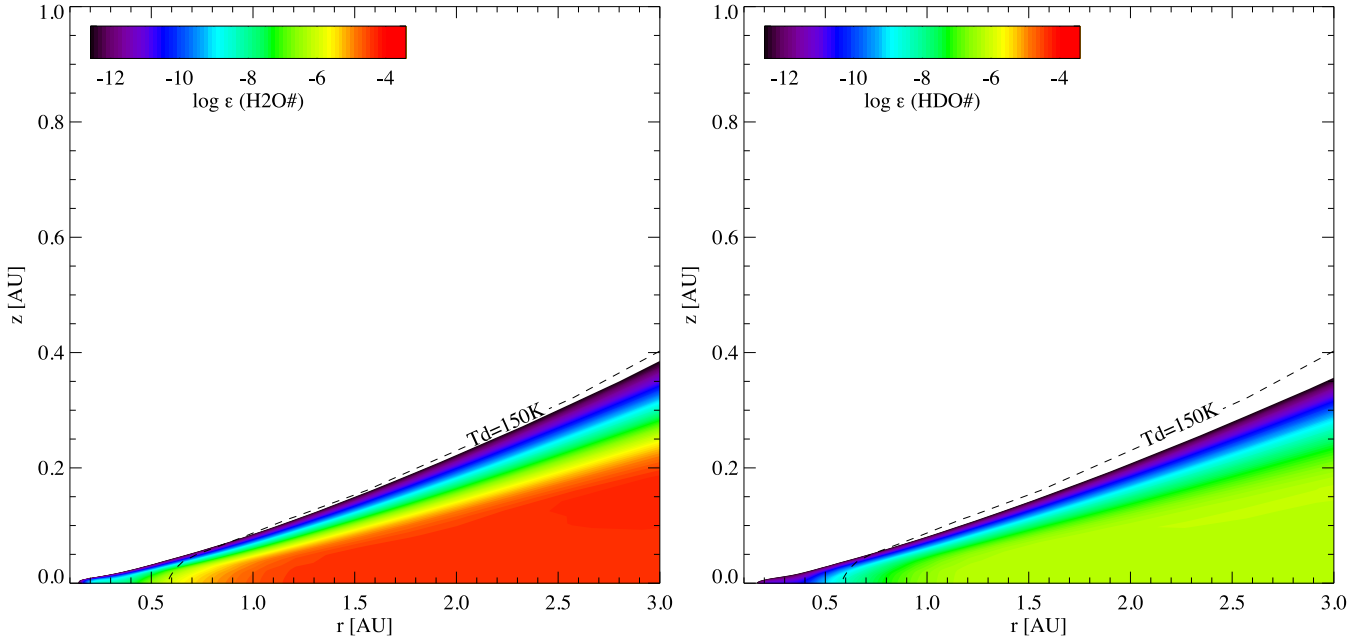


**Figure 5.** H<sub>2</sub>O and HDO ice abundance in the inner 3 AU. The dash-line indicate the region where the dust temperature is 150 K. H<sub>2</sub>O and HDO freeze at  $\sim 150$  K.

**Table 6.** Photodissociation and photoionisation reactions

	Reaction	q (s <sup>-1</sup> )	$\gamma$	Reference
$J_1$	H <sub>2</sub> + h $\nu$ $\rightarrow$ H + H	$3.4 \times 10^{-11}$	2.5	self-shielding factor, see text
$J_2$	HD + h $\nu$ $\rightarrow$ H + D	$2.6 \times 10^{-11}$	2.5	LePetit et al. 2002
$J_3$	CO + h $\nu$ $\rightarrow$ C + O	$2.0 \times 10^{-10}$	2.5	UMIST
$J_4$	OH + h $\nu$ $\rightarrow$ O + H	$3.5 \times 10^{-10}$	1.7	van Dishoeck 1988
$J_5$	OD + h $\nu$ $\rightarrow$ O + D	$4.0 \times 10^{-10}$	1.7	Crowell & Dalgarno 1985
$J_6$	H <sub>2</sub> O + h $\nu$ $\rightarrow$ H + OH	$5.9 \times 10^{-10}$	1.7	UMIST
$J_{7a}$	HDO + h $\nu$ $\rightarrow$ OH + D	–	–	$J_{7a} = 0.25J_6$ , see text
$J_{7b}$	HDO + h $\nu$ $\rightarrow$ OD + H	–	–	$J_{7b} = 0.75J_6$ , see text
$J_9$	C + h $\nu$ $\rightarrow$ C <sup>+</sup> + e			UMIST

Ref. UMIST: Woodall et al. (2007)

**Table 7.** Ion-neutral reactions

	Reaction	k (cm <sup>3</sup> s <sup>-1</sup> )	Reference
$k_{34}$	H <sup>+</sup> + D $\rightarrow$ D <sup>+</sup> + H	$1.0 \times 10^{-9} e^{-41/T}$	Watson (1976), UMIST
$k_{35}$	He <sup>+</sup> + H <sub>2</sub> $\rightarrow$ H + H <sup>+</sup> + He	$1.1 \times 10^{-13} (T/300)^{-0.24}$	UMIST
$k_{36}$	HD + H <sup>+</sup> $\rightarrow$ D <sup>+</sup> + H <sub>2</sub>	$1.0 \times 10^{-9} e^{-464/T}$	UMIST
$k_{37}$	H <sub>2</sub> + D <sup>+</sup> $\rightarrow$ H <sup>+</sup> + HD	$2.1 \times 10^{-9}$	UMIST
$k_{38}$	H + D <sup>+</sup> $\rightarrow$ H <sup>+</sup> + D	$1.0 \times 10^{-9}$	Watson (1976), UMIST
$k_{39}$	OH + C <sup>+</sup> $\rightarrow$ CO <sup>+</sup> + H	$7.7 \times 10^{-10}$	Prasad & Huntress (1980), UMIST
$k_{40}$	OD + C <sup>+</sup> $\rightarrow$ CO <sup>+</sup> + D	–	$k_{40} = k_{39}$ is assumed
$k_{41}$	He <sup>+</sup> + H <sub>2</sub> O $\rightarrow$ OH + He + H <sup>+</sup>	$6.0 \times 10^{-11}$	UMIST
$k_{42}$	He <sup>+</sup> + HDO $\rightarrow$ OD + He + H <sup>+</sup>	–	$k_{42} = 0.75k_{41}$ is assumed
$k_{43}$	He <sup>+</sup> + HDO $\rightarrow$ OH + He + D <sup>+</sup>	–	$k_{43} = 0.25k_{41}$ is assumed
$k_{44}$	He <sup>+</sup> + OH $\rightarrow$ O <sup>+</sup> + He + H	$1.1 \times 10^{-9}$	UMIST
$k_{45}$	He <sup>+</sup> + OD $\rightarrow$ O <sup>+</sup> + He + D	–	$k_{45} = k_{44}$ is assumed

Ref. UMIST: Woodall et al. (2007)

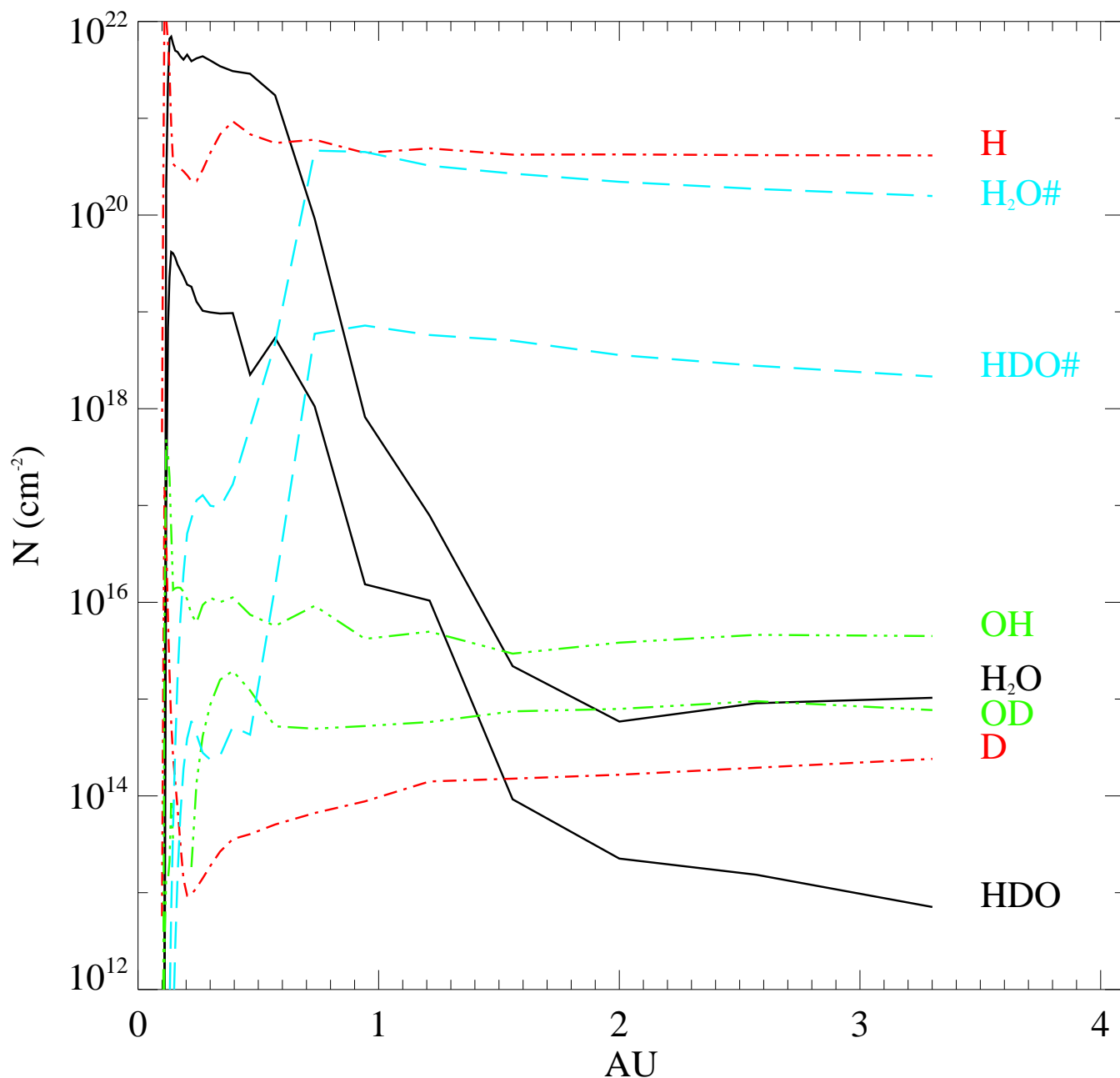


Figure 6. Half disc vertical column density for various species in the inner 3 AU.

- Charnley S. B., Tielens A. G. G. M., Rodgers S. D., 1997, *ApJL*, 482, L203+
- Crosswell K., Dalgarno A., 1985, *ApJ*, 289, 618
- Dartois E., Thi W.-F., Geballe T. R., Deboffle D., d'Hendecourt L., van Dishoeck E., 2003, *A&A*, 399, 1009
- Dorren J. D., Guinan E. F., 1994, *ApJ*, 428, 805
- Draine B. T., Bertoldi F., 1996, *ApJ*, 468, 269
- Drake M. J., 2005, *Meteoritics and Planetary Science*, 40, 519
- Genda H., Ikoma M., 2008, *Icarus*, 194, 42
- Gensheimer P. D., Mauersberger R., Wilson T. L., 1996, *A&A*, 314, 281
- Glassgold A. E., Meijerink R., Najita J. R., 2009, *ApJ*, 701, 142
- Gomes R., Levison H. F., Tsiganis K., Morbidelli A., 2005, *Nature*, 435, 466
- Guilloteau S., Piétu V., Dutrey A., Guélin M., 2006, *A&A*, 448, L5
- Hopkins M., Harrison T. M., Manning C. E., 2008, *Nature*, 456, 493
- Kamp I., Tilling I., Woitke P., Thi W., Hogerheijde M., 2009, *ArXiv e-prints*

**Table 8.** Cosmic-ray induced ionisation and recombination reactions ( $\zeta = 5 \times 10^{-17} \text{ s}^{-1}$ ).

Reaction	$k$ ( $\text{cm}^3 \text{ s}^{-1}$ )	Reference
$k_{\zeta,1}$ H + cr $\rightarrow$ H <sup>+</sup> + e <sup>-</sup>	$0.46 \times \zeta$	UMIST
$k_{\zeta,2}$ D + cr $\rightarrow$ D <sup>+</sup> + e <sup>-</sup>	$0.46 \times \zeta$	UMIST
$k_{\zeta,3}$ He + cr $\rightarrow$ He <sup>+</sup> + e <sup>-</sup>	$0.5 \times \zeta$	UMIST
$k_{\zeta,4}$ H <sub>2</sub> + cr $\rightarrow$ H <sup>+</sup> + H + e <sup>-</sup>	$0.04 \times \zeta$	UMIST
$k_{\zeta,5}$ HD + cr $\rightarrow$ H <sup>+</sup> + D + e <sup>-</sup>	–	$k_{\zeta,5} = 0.5k_{\zeta,4}$ is assumed
$k_{\zeta,6}$ HD + cr $\rightarrow$ D <sup>+</sup> + H + e <sup>-</sup>	–	$k_{\zeta,6} = 0.5k_{\zeta,4}$ is assumed
$k_{e^-,1}$ H <sup>+</sup> + e <sup>-</sup> $\rightarrow$ H + h $\nu$	$3.5 \times 10^{-12} (T/300)^{-0.70}$	Prasad & Huntress (1980)
$k_{e^-,2}$ D <sup>+</sup> + e <sup>-</sup> $\rightarrow$ D + h $\nu$	–	$k_{e^-,2} = k_{e^-,1}$ is assumed
$k_{e^-,3}$ He <sup>+</sup> + e <sup>-</sup> $\rightarrow$ He + h $\nu$	$4.5 \times 10^{-12} (T/300)^{-0.67}$	Prasad & Huntress (1980)
$k_{cp,1}$ OH + CRPhot $\rightarrow$ O + H	$1.3 \times 10^{-17} (509/(1-w))$	UMIST
$k_{cp,2}$ OD + CRPhot $\rightarrow$ O + D	$1.3 \times 10^{-17} (509/(1-w))$	$k_{cp,2} = k_{cp,1}$ is assumed
$k_{cp,3}$ H <sub>2</sub> O + CRPhot $\rightarrow$ OH + H	$1.3 \times 10^{-17} (971/(1-w))$	UMIST
$k_{cp,4}$ HDO + CRPhot $\rightarrow$ OD + H	$0.75 \times 1.3 \times 10^{-17} (971/(1-w))$	UMIST
$k_{cp,5}$ HDO + CRPhot $\rightarrow$ OH + D	$0.25 \times 1.3 \times 10^{-17} (971/(1-w))$	UMIST

Ref. UMIST: Woodall et al. (2007)

Le Petit F., Roueff E., Le Bourlot J., 2002, *A&A*, 390, 369Linsky J. L., 2003, *Space Science Reviews*, 106, 49Lyons J. R., Young E. D., 2005, *Nature*, 435, 317Morbidelli A., Chambers J., Lunine J. I., Petit J. M., Robert F., Valsecchi G. B., Cyr K. E., 2000, *Meteoritics and Planetary Science*, 35, 1309Nuth J. A., 2008, *Earth Moon and Planets*, 102, 435Parise B., Caux E., Castets A., Ceccarelli C., Loinard L., Tielens A. G. G. M., Bacmann A., Cazaux S., Comito C., Helmich F., Kahane C., Schilke P., van Dishoeck E., Wakelam V., Walters A., 2005, *A&A*, 431, 547Parise B., Simon T., Caux E., Dartois E., Ceccarelli C., Rayner J., Tielens A. G. G. M., 2003, *A&A*, 410, 897Prasad S. S., Huntress Jr. W. T., 1980, *ApJS*, 43, 1Raymond S. N., Quinn T., Lunine J. I., 2004, *Icarus*, 168, 1Raymond S. N., Quinn T., Lunine J. I., 2005, *ApJ*, 632, 670Richet P., Bottinga Y., Janoy M., 1977, *Annual Review of Earth and Planetary Sciences*, 5, 65Righter K., Drake M. J., Scott E. R. D., 2006, *Compositional Relationships Between Meteorites and Terrestrial Planets. Meteorites and the Early Solar System II*, pp 803–828Robert F., Gautier D., Dubrulle B., 2000, *Space Science Reviews*, 92, 201Roberts H., Herbst E., Millar T. J., 2004, *A&A*, 424, 905Roberts H., Millar T. J., 2000, *A&A*, 361, 388Salyk C., Pontoppidan K. M., Blake G. A., Lahuis F., van Dishoeck E. F., Evans II N. J., 2008, *ApJL*, 676, L49Shafer N., Satyapal S., Bersohn R., 1989, *J. Chem Phys.*, 90, 6807Stimpfl M., Walker A. M., Drake M. J., de Leeuw N. H., Deymier P., 2006, *Journal of Crystal Growth*, 294, 83Thi W.-F., Bik A., 2005, *A&A*, 438, 557Tielens A. G. G. M., 2005, *The Physics and Chemistry of the Interstellar Medium. The Physics and Chemistry of the Interstellar Medium*, by A. G. G. M. Tielens, pp. . ISBN 0521826349. Cambridge, UK: Cambridge University Press, 2005.van Dishoeck E. F., 1988, in Millar T. J., Williams D. A., eds, *Rate Coefficients in Astrochemistry. Proceedings of a Conference held in UMIST, Manchester, United Kingdom, September 21-24, 1987*. Editors, T.J. Millar, D.A. Williams; Publisher, Kluwer Academic Publishers, Dordrecht, Boston, 1988. ISBN # 90-277-2752-X. LC # QB450 .R38 1988. P. 49, 1988 Photodissociation and Photoionization Processes. pp 49–+van Dishoeck E. F., Dalgarno A., 1984, *ApJ*, 277, 576van Dishoeck E. F., Jonkheid B., van Hemert M. C., 2008, *Faraday Discussion of the Chemical Society*, 133, 231Vander Wal R. L., Scott J. L., Crim F. F., 1990, *J. Chem Phys.*, 92, 803Vander Wal R. L., Scott J. L., Crim F. F., Weide K., R. S., 1991, *J. Chem Phys.*, 94, 3548Visser R., van Dishoeck E. F., Doty S. D., Dullemond C. P., 2009, *A&A*, 495, 881Watson W. D., 1976, *Reviews of Modern Physics*, 48, 513Willacy K., Woods P. M., 2009, *ApJ*, 703, 479Woitke P., Kamp I., Thi W.-F., 2009, *A&A*, 501, 383Woitke P., Thi W.-F., Kamp I., Hogerheijde M. R., 2009, *A&A*, 501, L5Woodall J., Agúndez M., Markwick-Kemper A. J., Millar T. J., 2007, *A&A*, 466, 1197



Yung Y. L., Wen J.-S., Pinto J. P., Pierce K. K., Allen M., 1988, *Icarus*, 76, 146  
Zhang J. Z., Imre D. G., 1988, *Chem. Phys. Lett.*, 149, 233

This paper has been typeset from a  $\text{T}_{\text{E}}\text{X}/\text{L}_{\text{A}}\text{T}_{\text{E}}\text{X}$  file prepared by the author.